



Inhibiting the soluble epoxide hydrolase increases the EpFAs and ERK1/2 expression in the hippocampus of LiCl-pilocarpine post-status epilepticus rat model

Weifeng Peng^{a,b,c,*}, Zihan Hu^c, Yijun Shen^a, Xin Wang^c

^a Department of Neurology, Shanghai Geriatric Medical Center, Shanghai, China

^b Department of Neurology, Zhongshan Hospital Fudan University Xiamen Branch, Xiamen, China

^c Department of Neurology, Zhongshan Hospital Fudan University, Shanghai, China

ARTICLE INFO

Keywords:

Epilepsy
Soluble epoxide hydrolase
Epoxygenated fatty acids (EpFAs)
Extracellular signal-activated protein kinase 1/2 (ERK1/2)

ABSTRACT

Purpose: This study aimed to investigate the enzyme activity of soluble epoxide hydrolase (sEH) and quantify its metabolic substrates, namely epoxygenated fatty acids (EpFAs), and products of sEH in the hippocampus after administering TPPU [1-trifluoromethoxyphenyl-3-(1-propionylpiperidin-4-yl)urea], an inhibitor of sEH. Furthermore, it explored whether the extracellular signal-activated protein kinase 1/2 (ERK1/2) is involved in the anti-seizure effects of TPPU in the lithium chloride (LiCl)-pilocarpine induced post-status epilepticus (SE) rat model.

Methods: The rats were intraperitoneally (I.P.) injected with LiCl and pilocarpine to induce SE and then spontaneous recurrent seizures (SRS) were observed. Rats were randomly assigned into SRS + TPPU group (intragastrically administering 0.1 mg/kg/d TPPU), SRS + Vehicle group (administering the vehicle instead), and Control group. Enzyme-linked immunosorbent assay, Western-blot analysis, and ultra-high-performance liquid chromatography/mass spectrometry (LC/MS) were performed to measure the enzyme activity of sEH, the protein level of sEH and ERK1/2, and the concentration of TPPU and polyunsaturated fatty acids (PUFAs) metabolisms in the hippocampus.

Results: The frequency of SRS events of Racine stage 3 or higher ranged from 0 to 19 per week in the SRS + Vehicle group, compared to 0–5 per week in the SRS + TPPU group. sEH enzyme activity and protein levels were significantly elevated in the SRS + Vehicle group compared to the Control group. After TPPU administration, the hippocampal TPPU concentration reached 10.94 ± 4.37 nmol/kg. sEH enzyme activity was significantly reduced in the LiCl-pilocarpine-induced post-SE rat model, although sEH protein levels did not decrease significantly. The regioisomers 8,9-, 11,12-, and 14,15-EETs, total EETs, the EETs/DHETs ratio, other EpFAs including 16(17)-EpDPA, and the 19(20)-EpDPA/19,20-DiHDPA ratio in the hippocampus were significantly increased. Additionally, the p-ERK1/2 to ERK1/2 ratio in the hippocampus was significantly elevated following TPPU administration.

Conclusion: This study demonstrates that inhibiting sEH with TPPU increases the levels of EETs, other EpFAs, and ERK1/2 expression in the hippocampus of a LiCl-pilocarpine-induced post-SE rat model. These findings suggest that the anti-seizure effect of TPPU may be mediated through the EETs-ERK1/2 pathway.

1. Introduction

Epilepsy is a chronic brain disorder characterized by recurrent seizures and neuropsychiatric comorbidities that significantly impair the quality of life for affected individuals (Josephson et al., 2017). However,

the mechanisms underlying epileptogenesis remain unclear. Increasing evidence from both human patients and animal models suggests that neuroinflammation plays a substantial role in the development of epilepsy (Vezzani et al., 2013; Butler et al., 2016). During the process of epileptogenesis, proinflammatory cytokines, such as interleukin (IL)-1 β ,

* Correspondence to: Department of Neurology, Shanghai Geriatric Medical Center, Zhongshan Hospital, Fudan University, 2560 Chun-Shen Road, Shanghai 201104, China.

E-mail address: peng.weifeng@zs-hospital.sh.cn (W. Peng).

<https://doi.org/10.1016/j.ibneur.2024.10.001>

Received 7 August 2024; Received in revised form 27 September 2024; Accepted 10 October 2024

Available online 11 October 2024

2667-2421/© 2024 The Author(s). Published by Elsevier Inc. on behalf of International Brain Research Organization. This is an open access article under the CC BY-NC-ND license (<http://creativecommons.org/licenses/by-nc-nd/4.0/>).

IL-6, tumor necrosis factor- α (TNF- α), and prostaglandin E2 (PGE2), are produced in excess (Vezzani et al., 2008; Wang et al., 2018). Therefore, anti-inflammatory treatment may represent an optimal therapeutic strategy for patients with epilepsy (Paudel et al., 2018).

Epoxide hydrolases (EHs) are proteins that catalyze the conversion of epoxides to diols through the addition of water (Morisseau and Hammock, 2005). There are several types of EHs, including microsomal epoxide hydrolase (mEH), soluble epoxide hydrolase (sEH), and cholesterol EH, among others. Of these, sEH is widely expressed in various human tissues and is thought to play a role in the inflammatory process (Morisseau and Hammock, 2013). Epoxygenated fatty acids (EpFAs), including epoxyeicosatrienoic acids (EETs), are endogenous substrates for sEH derived from polyunsaturated fatty acids (PUFAs) such as arachidonic acid (ARA), eicosapentaenoic acid (EPA), linoleic acid (LA), and docosahexaenoic acid (DHA). ARA, LA, EPA, and DHA are abundantly stored in membrane phospholipids and are metabolized into active intermediates by cyclooxygenases (COX), lipoxygenases (LOX), and cytochrome P450 (CYP450) epoxygenases. Among these, CYP450 epoxygenases convert ARA into various subtypes of EETs and other EpFAs (Swardfager et al., 2018). Studies have demonstrated that EETs possess anti-inflammatory and neuroprotective effects (Lliff et al., 2010). However, EETs are hydrolyzed by sEH and converted into their respective diols, such as dihydroxyeicosatetraenoic acids (DHETs), which are reported to be mostly inactive or even detrimental in regulating inflammation (Hu et al., 2017).

In mammals, the sEH protein is a 125 kDa dimer composed of two identical 62 kDa monomers (Morisseau and Hammock, 2013). It is highly expressed and distributed throughout the central nervous system, including various brain regions such as the cerebral cortex, hippocampus, amygdala, and striatum (Sura et al., 2008). At the microstructural level, sEH exhibits cell type-specific localization, found in the soma and processes of neuronal cells, astrocytes, oligodendrocytes, and microvascular endothelial cells in the brain (Bianco et al., 2009). Studies indicate that sEH is involved in the pathological processes of neurological diseases (Hashimoto, 2019). For instance, in a study involving 20 patients who underwent anterior temporal lobe resection due to temporal lobe epilepsy, the level of sEH was significantly higher in the temporal cortex of patients with epilepsy compared to the control group (Ahmedov et al., 2017). Inhibitors of sEH have demonstrated anticonvulsant effects on spontaneous recurrent seizures (SRS) and antidepressant effects on epilepsy-associated depression in pilocarpine-induced rodent epilepsy models (Shen et al., 2019; Hung et al., 2015).

Although these studies have shown increased protein levels of sEH in the hippocampus of pilocarpine rodent epilepsy models, the enzyme activity of sEH and the changes in the levels of its substrates and products in the brain remain undetermined. Therefore, in this study, we aimed to investigate the enzyme activity of sEH and quantify the metabolic substrates of polyunsaturated fatty acids (PUFAs), specifically epoxygenated fatty acids (EpFAs), as well as the products of sEH in the hippocampus after administering TPPU [1-trifluoromethoxyphenyl-3-(1-propionylpiperidin-4-yl)urea], an sEH inhibitor. We also sought to explore whether the extracellular signal-regulated kinase 1/2 (ERK1/2) pathway is involved in the anti-seizure effect of TPPU in a LiCl-pilocarpine-induced post-status epilepticus rat model.

2. Methods

2.1. Animals

Male adult Sprague-Dawley rats aged 6–8 weeks and weighing 200–250 g (Shanghai Charles River Laboratory) were used in this study. They were raised 4/cage at 22–25°C and under a 12 h day-night cycle. The experiment was approved by the Committee of Animal Care and Use in Zhongshan Hospital of Fudan University (Shanghai, China) and conformed to the guidelines of the National Institutes of Health.

Measures were taken to reduce the number of animals used, and efforts were made to minimize animal suffering.

2.2. Establishment of the LiCl-pilocarpine-induced post-SE rat model and grouping

As described previously (Peng et al., 2016), rats were intraperitoneally injected (I.P.) LiCl (127 mg/kg, dissolved in water, Sigma, St. Louis, MO, USA), scopolamine methyl bromide (1 mg/kg, Sigma-Aldrich, USA), and muscarinic agonist pilocarpine (40 mg/kg, Sigma-Aldrich, USA) sequentially at intervals of 24 h and 30 min respectively. The seizure severity was evaluated by the modified Racine scale (Racine, 1972). The standard of SE in this study was defined as sustained recurrent seizures greater than or equal to Racine stage 4 for 30 min. At 30 min after seizure onset, rats meeting the standard of SE were treated with diazepam (10 mg/kg, Tianjin, China) to terminate seizures. One week after SE induction, the survived rats were monitored with a video surveillance system (a CCD camera, JVC, Japan) to observe SRS. Six-weeks monitoring period (from the onset of the 2nd week to the end of the 7th week after SE induction) with 6 h/d was conducted. The frequency of SRS reaching a Racine stage 3–5 (rearing and/or rearing and falling) were counted.

The rats of LiCl-pilocarpine induced post-SE model were divided into two groups randomly according to administration of TPPU (dissolved in a saline solution containing 40 % polyethylene glycol 400, PEG 400, at 0.1 mg/kg/d) or not: the SRS + TPPU group and the SRS + Vehicle group. TPPU was given for 4 weeks from the 21st day to 49th day after SE induction by gastric gavage at 8 am every morning (Liu et al., 2013). The SRS + Vehicle group was given the vehicle (PEG 400) instead of TPPU and the Control group was simply given LiCl and PEG 400. At 7w after SE induction, the brain tissues were harvested.

2.3. Tissue preparation and protein extraction

The brain tissues were taken out after rats were deeply anesthetized with 4 % chloral hydrate and euthanized by cervical dislocation. The hippocampi of rats were carefully dissected out and put into 4°C phosphate-buffered saline (PBS). The tissue protein extraction reagent (Beyotime Institute of Biotechnology, China) containing EDTA-free complete protease inhibitors (Beyotime, China) was used to extract total protein from the hippocampi of rats, and the Bio-Rad protein assay kit (Beyotime, China) was adopted to measure total protein concentration.

2.4. Enzyme-linked immunosorbent assay (ELISA)

The enzyme activity of sEH in the hippocampi of rats was measured using the Soluble Epoxide Hydrolase Inhibitor Screening Assay Kit (Cayman Chemical). The procedures were as follows: 1) adding 190 μ L of assay buffer and 5 μ L cell lysis buffer to a well for the background; 2) Five concentration gradients of the standard sEH sample were set, 0.5, 1, 2, 4, 8 μ L standard samples were placed into the well A1–5, add 5 μ L cell lysis buffer, and add some assay buffer to make the volume into 195 μ L; 3) other wells for samples were added into 10 μ L samples and 185 μ L assay buffer; 4) incubating for 2 hours at room temperature (RT) on a shaker at 800 rpm; 5) the liquid was removed and then 100 μ L wash buffer were put into wells and washed for three times; 6) covering, and incubating for 1 h at RT on the shaker at 800 rpm, washing was repeated as before; 7) adding 50 μ L of diluted streptavidin-PE to each well, incubating for 30 minutes at RT on the shaker at 800 rpm, and repeating the wash again; 8) 100 μ L of wash buffer was added to each well, covered, and incubated for 2 min at RT on the shaker at 800 rpm. A Luminex analyser was used to read the results within 90 min.

2.5. Western blot analysis

The expression level of ERK1/2 in the hippocampi of rats was measured by the Western-blot analysis. Sodium dodecyl sulphate-polyacrylamide gel electrophoresis (SDS-PAGE) was used to separate total proteins, which was transferred to cellulose acetate membranes. After that, the membranes were blocked and incubated with primary antibodies i.e. rabbit anti-ERK1/2 (42/44 kDa, 1:1000, CST) and rabbit anti-sEH (63 kDa, 1:500, ABclonal) at 4°C. The rabbit anti-β-actin primary antibody (40 kDa, 1:1000, Beyotime) was set as the internal reference. The membrane was washed with 4°C PBS (10 mM, pH 7.4) after incubation for 24 h, and then it was incubated with the goat anti-rabbit IgG secondary antibody (1:1000, Beyotime) for 2 h at RT. Quantitative analysis of target proteins bands was conducted by Tanon Image software (version 4100, Shanghai, China). The optical density (OD) value of each sample was normalized by the corresponding amount of β-actin.

2.6. The ultra-high-performance liquid chromatography/mass spectrometry (LC/MS) method

The homogenate of rat hippocampus was prepared by using a solid phase extraction (SPE) method. The sample mixed with SPE solution etc. and pass through the cartridges by gravity. The cartridges were washed with the 2 ml SPE solution, dried under vacuum for 5 min, and then eluted with ethyl acetate (EtOAc, 1.5 ml) into 2 ml tubes each containing 30 % glycerol in MeOH (5 μL) on the bottom as a trap solution. The volatile solvents were removed from the tubes by using a SpeedVac concentrator (Thermo Scientific) until the glycerol remained on the bottom. The residue was formulated with IS II solution (50 μL), strongly mixed on a vortex mixer for 5 min, and then centrifuged at 11200 × g for 5 min under 4°C. The entire supernatant was transferred into an ultra-free centrifugal filter. After centrifuging at 11200 × g for 5 min under 4°C, the filtrate was then transferred into a 150 μL insert fixed in a 2 ml vial and stored at –20°C until analysis.

The concentrations of TPPU and PUFAs metabolisms were analysed by established liquid chromatography electrospray ionization tandem mass spectrometry method reported by Luo et al. (2019a); Luo et al. (2019b). Specifically, chromatographic separation was performed on an Agilent 1260 Infinity liquid chromatography instrument equipped with a 2.1 × 150 mm ZORBAX Eclipse Plus C18 1.8 μm column held at 50 °C. The solvent system consisted of water/AA (999/1 v/v, solvent A) and ACN /MeOH/AA (840/159/1 v/v; solvent B). The injection volume was 10 μL. The samples were kept at 4 °C in the autosampler. Analytes were monitored by negative mode electrospray ionization tandem mass spectrometry in MRM mode on an AB Sciex QTrap6500 Mass Spectrometer (AB Sciex, Framingham, MA). The gas flow rate was fixed for curtain gas, ion source gas 1 and ion source gas 2 as 35, 50, 50 L/h, respectively. The collision gas was set as medium. Electrospray ionization was performed with an IonSpray Voltage set at –4500 V and the source temperature was set at 500 °C.

2.7. Statistical analysis

The Graphpad Prism 7 software was used to conduct the statistical analysis in this study. Comparisons between groups were performed using the Student's t-test, one-way analysis of variance (ANOVA), and the non-parametric Mann-Whitney U test. For one-way ANOVA, a post-hoc Tukey test was applied for pairwise comparisons. A P value of less than 0.05 was considered statistically significant. Data are expressed as mean ± standard deviation (SD).

3. Results

3.1. SRS observation in the LiCl-pilocarpine-induced post-SE rat model

As described in the earlier article (Shen et al., 2019), rats induced SE by I.P. administering LiCl-pilocarpine were video-monitored for 7w to observe SRS. Fourteen rats having observed SRS at 2w after SE were included, of which 7 rats each were randomly assigned to SRS + Vehicle and SRS + TPPU groups. There was no difference in the latency of inducing SE between the two groups (14.25 ± 3.3 min SRS + Vehicle group vs. 14.5 ± 2.38 min in SRS + TPPU group, $P > 0.05$). The seizure frequency of SRS that equal to or greater than Racine 3 degree ranged from 0 to 19 (median, 3) every week in SRS + Vehicle group comparing to 0–5 (median, 1) every week in SRS + TPPU group (Mann-whitney U test, $P < 0.001$).

3.2. The levels of sEH protein and sEH enzyme activity in the hippocampus were compared between the LiCl-pilocarpine-induced post-SE rat model and Control group

After 7 weeks of observation following SE induction, the hippocampi of the rats were removed for measurement. Quantitative measurement of sEH protein was performed by the Western-blot method. The level of sEH protein in the hippocampus was significantly increased in the LiCl-pilocarpine-induced post-SE rat model (SRS + Vehicle group) compared with Control group (Fig. 1, $*P < 0.05$).

The enzyme activity of sEH in the hippocampus measured by ELISA was compared between the SRS + Vehicle and Control groups. The result showed that the enzyme activity of sEH was significantly increased in the SRS + Vehicle group compared with Control group (see Fig. 2).

3.3. TPPU administration increased EpFAs and the ratios of sEH substrates and products in the hippocampus of LiCl-pilocarpine-induced post-SE rat model

The concentration of TPPU was measured by the LC/MS method in the hippocampus, which was 10.94 ± 4.37 nmol/kg in the SRS + TPPU group compared with blank in the SRS + Vehicle and Control groups. Simultaneously, the enzyme level of sEH was significantly decreased after TPPU administration in the SRS + TPPU group compared with the SRS + Vehicle group ($*P < 0.05$, see Fig. 2), however, the protein level of sEH did not decrease significantly (see Fig. 1).

Next, the PUFAs metabolic substrates and products of sEH in the hippocampus were measured through the LC/MS method in this study either. As shown in Fig. 3, the diagram depicts the metabolic profiles of PUFAs including ARA, LA, and DHA in this study. The PUFAs are metabolized by CYP450 epoxygenases into different subtypes of EETs, epoxyoctadecamonoenoic acid (EpOMEs), and epoxydocosapentaenoic acid (EpDPAs), which are the substrates of sEH. They are further metabolized by sEH into the products including dihydroxyicosatrienoic acid (DHETs), dihydroxy octadecamonoenoic acid (DHOMEs), and dihydroxydocosapentaenoic acid (DiHDPA), respectively. As listed in Table 1, the concentrations of PUFAs metabolic substrates and products of sEH measured in this study were compared among the SRS + Vehicle, SRS + TPPU, and Control groups ($*P < 0.05$, $**P < 0.01$). The regioisomers 8,9-, 11,12-, and 14,15-EETs, the sums of EETs, and the ratio of EETs/DHETs in the hippocampus was significantly increased in the SRS + TPPU group compared with SRS + Vehicle group ($*P < 0.05$, $**P < 0.01$, Fig. 4A). In addition, the level of other EpFAs including EpOMEs and EpDPA in the hippocampus could also be detected in this study, and it showed that 16(17) EpDPA and the ratio of 19(20)-EpDPA/19,20-DiHDPA were both significantly increased in the SRS + TPPU group compared with SRS + Vehicle group ($*P < 0.05$, $**P < 0.01$, Fig. 4B), while no difference in the ratio of EpOMEs/DHOMEs was found after administering TPPU.

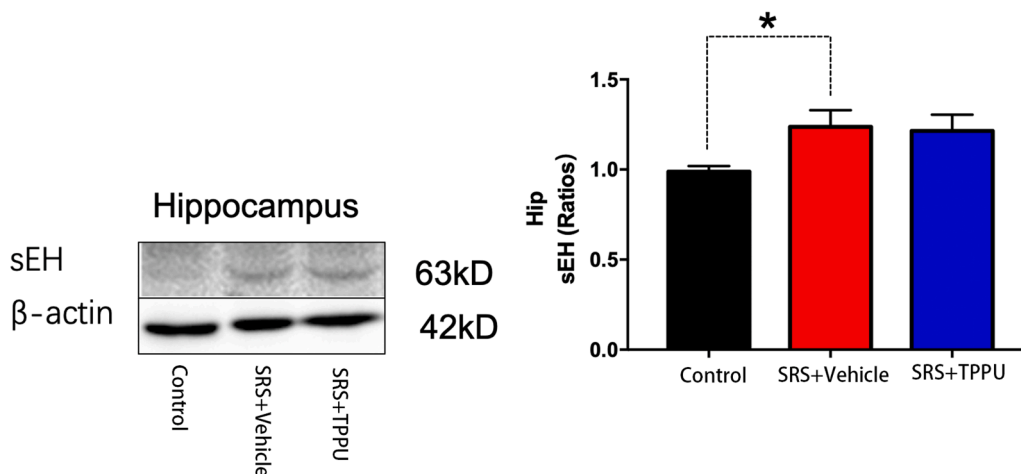


Fig. 1. In the hippocampus, the expression level of sEH protein, measured by Western blot analysis seven weeks after seizure induction, was significantly increased in the LiCl-pilocarpine-induced post-status epilepticus rat model (SRS + Vehicle group) compared to the control group (n = 7 in every group, F=3.75, df=18, *P<0.05).

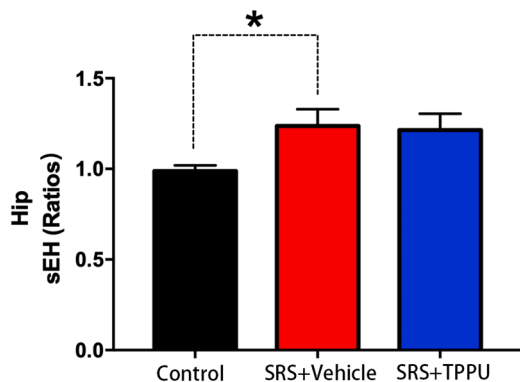


Fig. 2. The enzyme activity of sEH (IU/ml) was significantly increased in the SRS + Vehicle group compared to the Control group, and it was significantly decreased in the SRS + TPPU group compared to the SRS + Vehicle group (n = 7 in every group, F=29.5, df=18, *P<0.01).

3.4. The expression of ERK1/2 was significantly increased in the hippocampus of LiCl-pilocarpine-induced post-SE rat model after TPPU administration

The expression level of ERK1/2 and its phosphorylated form was measured by the Western-blot method. As shown in Fig. 5, the result showed that the ratio of p-ERK1/2 to ERK1/2 was significantly increased in the SRS + TPPU group compared with SRS + Vehicle (*P<0.05).

4. Discussion

In this study, we observed that both the expression of sEH protein and the enzyme activity of sEH were significantly elevated in the hippocampus of the LiCl-pilocarpine-induced post-SE rat model compared to the control group. After administering TPPU, sEH enzyme activity decreased, while the levels of PUFAs metabolic substrates, including EpFAs, and the ratios of substrates to products increased in the hippocampus of the post-SE rat model. This finding suggests that TPPU may exert its anti-seizure effects through the cellular mechanisms involving sEH metabolic substrates, particularly EETs. Additionally, the increased expression of ERK1/2 in the hippocampus indicates its potential role in

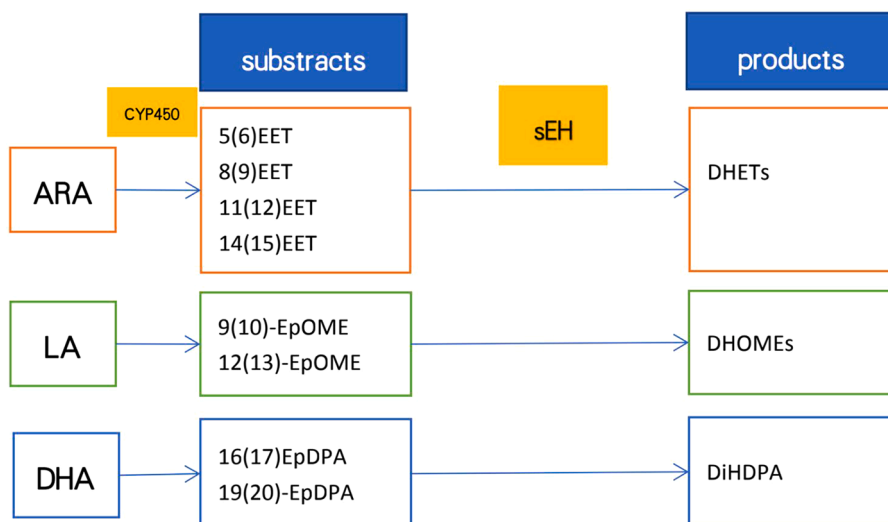


Fig. 3. A simplified cascade illustrating the metabolism of polyunsaturated fatty acids (PUFAs), including arachidonic acid (ARA), linoleic acid (LA), and docosahexaenoic acid (DHA), through the cytochrome P450 epoxygenase and soluble epoxide hydrolase (sEH) pathways.

Table 1

Comparative Analysis of TPPU and Metabolic Substrates and Products of sEH in the Hippocampus of LiCl-Pilocarpine-Induced Post-SE Rat Model and Controls.

Measuring items (nmol/kg)	Control group (n=7)	SRS + Vehicle group (n=7)	SRS + TPPU group (n=7)	P value (ANOVA test post-hoc analysis, SRS + Vehicle vs. SRS + TPPU)
TPPU	NA	NA	10.94 ± 4.37	NA
14(15) EET	32.72 ± 7.73	31.01 ± 9.03	60.79 ± 31.49	0.026
11(12) EET	26.53 ± 6.94	22.41 ± 9.07	40.97 ± 15.65	0.016
8(9) EET	20.83 ± 4.83	15.76 ± 4.40	31.86 ± 12.60	0.005
5(6) EET	47.16 ± 11.09	39.14 ± 12.25	57.23 ± 15.91	0.05
9(10)-EpOME	8.44 ± 7.13	4.81 ± 1.59	6.72 ± 1.63	0.692
12(13)-EpOME	19.42 ± 13.72	12.42 ± 3.92	17.47 ± 3.09	0.514
Sum (EETs)	127.24 ± 29.88	108.32 ± 33.44	190.85 ± 73.63	0.016
Sum (DHETs)	3.10 ± 0.82	3.34 ± 1.85	2.69 ± 0.72	0.598
EETs/DHETs	43.23 ± 14.64	38.25 ± 15.86	71.70 ± 21.38	0.006
Sum (EpOMEs)	27.86 ± 20.71	17.23 ± 5.37	24.19 ± 4.08	0.047
Sum (DHOMEs)	7.41 ± 2.89	5.34 ± 3.40	4.91 ± 2.35	0.96
EpOMEs/DHOMEs	3.51 ± 1.75	5.10 ± 3.92	5.86 ± 2.67	0.879
16(17) EpDPA	2.52 ± 0.65	2.18 ± 0.80	4.93 ± 2.13	0.004
19(20)-EpDPA/19,20-DiHDPA	1.75 ± 1.02	0.31 ± 0.11	2.43 ± 1.73	0.008

DHET: dihydroxyeicosatrienoic acid; DHOME: dihydroxy octadecamonoenoic acid; DiHDPA: dihydroxydocosapentaenoic acid; EET: epoxyeicosatrienoic acid; EpDPA: epoxydocosapentaenoic acid; EpOME: epoxyoctadecamonoenoic acid; NA: not applicable; SE: status epilepticus; sEH: soluble epoxide hydrolase; SRS: spontaneous recurrent seizure; TPPU: 1-trifluoromethoxyphenyl-3-(1-propionylpiperidin-4-yl) urea

the cellular mechanisms of EETs within the LiCl-pilocarpine-induced post-SE rat model.

In our previous study, we found that administering TPPU in the LiCl-pilocarpine-induced post-SE rat model reduced the frequency of spontaneous recurrent seizures (SRS) and alleviated epilepsy-associated depressive behaviors in the rats (Shen et al., 2019). Similarly, a study by Hung et al. confirmed that TPPU, the sEH inhibitor, exhibited anti-seizure effects in two mouse models of temporal lobe epilepsy induced by either pilocarpine or electrical amygdala kindling (Hung et al., 2015). Additionally, Vito et al. demonstrated that the sEH inhibitor had anti-inflammatory effects and prevented mortality induced by tetramethylenedisulfotetramine (a potent convulsant poison) in mice when combined with diazepam (Vito et al., 2014). The behavioral observations in this study showed a decrease in the frequency of SRS following TPPU administration, which is consistent with previous findings.

The sEH is one of the key enzymes responsible for hydrolyzing EETs and other metabolites derived from PUFAs, which are predominantly stored in membrane phospholipids. This study demonstrates that sEH is widely expressed in the central nervous system (Sura et al., 2008). Increased expression of sEH protein has been associated with various neurological and psychiatric diseases, including epilepsy, Parkinson's disease, Alzheimer's disease, depression, bipolar disorder, schizophrenia, and autism spectrum disorders (Swardfager et al., 2018; Ahmedov et al., 2017; Grinan-Ferre et al., 2020; Ma et al., 2019; Zarriello et al., 2019). However, the enzyme activity of sEH has yielded

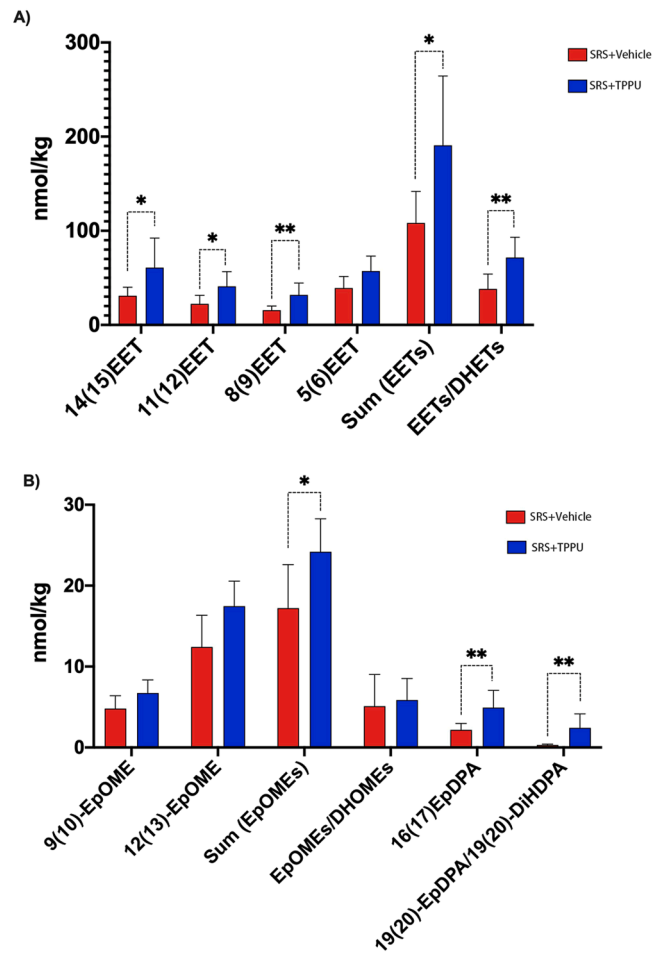


Fig. 4. A) The levels of regioisomers 8,9-, 11,12-, and 14,15-EETs, as well as the total EETs and the ratio of EETs to DHETs in the hippocampus, were significantly increased in the SRS + TPPU group compared to the SRS + Vehicle group (* $P < 0.05$, ** $P < 0.01$). B) The levels of other EpFAs, including EpOMEs, 16(17) EpDPA, and the ratio of 19(20)-EpDPA to 19,20-DiHDPA were also significantly elevated in the SRS + 0.1 TPPU group compared to the SRS + Vehicle group ($n = 7$ in each group; * $P < 0.05$, ** $P < 0.01$).

somewhat controversial results (Ren et al., 2016). In our previous study, we found that sEH protein expression was significantly elevated in the prefrontal cortex and hippocampus of the LiCl-pilocarpine-induced post-SE rat model (Shen et al., 2019). In this study, we further demonstrated that both the expression of sEH and its enzyme activity were significantly increased in the hippocampus of this model. After administering TPPU, we observed a significant decrease in sEH enzyme activity, while no significant change was noted in the expression of sEH protein. These findings suggest that the action of TPPU primarily reduces sEH enzyme activity without affecting sEH protein levels, which may be influenced by various other pathological factors.

Several sEH inhibitors have been developed in recent years, including 12-(3-adamantan-1-yl-ureido)-dodecanoic acid (AUDA), 1-adamantan-1-yl-3-(5-(2-(2-ethoxyethoxy)ethoxy)pentyl)urea (AEPU), trans-4-(4-(3-adamantan-1-yl-ureido)-cyclohexyloxy)-benzoic acid (t-AUCB), and TPPU, among others (Swardfager et al., 2018). Ideal sEH inhibitors should exhibit maximal bioavailability, longer half-lives, higher maximum drug concentrations in the blood (C_{max}), and larger area under the curve (AUC) (Zarriello et al., 2019). Additionally, for drugs targeting the central nervous system, it is crucial that they effectively cross the blood-brain barrier (BBB). Studies have shown that TPPU is a potent sEH inhibitor with sufficient solubility in water, extensive systemic distribution to tissues, and the ability to cross the

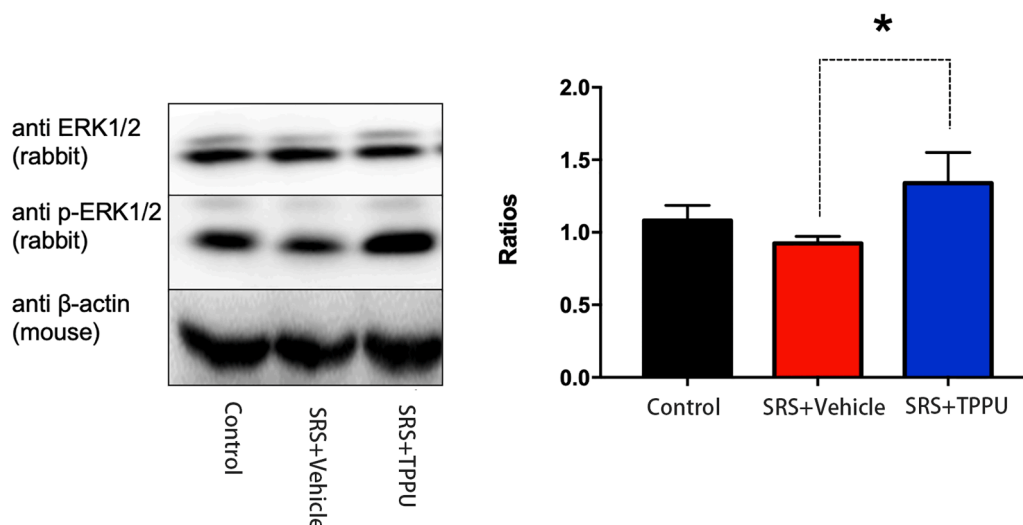


Fig. 5. The ratio of p-ERK1/2 to ERK1/2 was significantly increased in the SRS + TPPU group compared to the SRS + Vehicle group ($n=7$ in every group, $F=13.55$, $df=18$, $*P<0.05$).

BBB effectively, whether administered via intraperitoneal injection or orally (Ren et al., 2016; Ulu et al., 2016). In this study, TPPU was administered to rats via intragastric administration. We measured the concentration of TPPU in the hippocampus using the LC/MS method and found that the concentration was significantly elevated compared to the blank controls, indicating excellent gastric absorption and BBB permeability of TPPU.

The anti-seizure effect of TPPU may be attributed by the elevation of EETs and other EpFAs. In this study, we found that the total levels of EETs, the ratio of EETs to DHETs, as well as the individual EETs (14(15) EET, 11(12) EET, and 8(9) EET) were significantly increased in the hippocampus of the LiCl-pilocarpine-induced post-SE rat model following TPPU administration. However, no significant difference was observed in the levels of 5(6) EET between the SRS + TPPU and SRS + Vehicle groups. Additionally, other EpFAs, including EpOMEs, 16(17) EpDPA, and 19(20) EpDPA derived from LA and DHA, were also significantly elevated in the hippocampus after TPPU treatment. A previous study indicated that co-injection of the sEH inhibitor with EETs—but not with epoxy-DHA or epoxy-EPA—into the brains of mice delayed the onset of pentylenetetrazol-induced seizures, which supports the crucial role of EETs in mediating the anti-seizure effects (Inceoglu et al., 2013).

Under physiological conditions, endogenous EETs play important roles in various cellular actions, including the regulation of cerebral blood flow, neurohormone release, and synaptic transmission in the brain (Iliff et al., 2010). How the levels of EETs change in the pathophysiological states of neurological and psychiatric diseases have not been fully elucidated. In this study, we did not find any differences in the levels of EETs and other EpFAs in the hippocampus of the LiCl-pilocarpine-induced post-SE rat model compared to the control group. Under pathological conditions, membrane phospholipids may be damaged, leading to the release of PUFAs from membrane lipids, which are then metabolized through the COX, LOX, CYP hydroxylase, and CYP epoxygenase pathways (Kihara, 2020). This suggests that the levels of EETs and other EpFAs may be influenced by multiple factors, rather than solely by sEH activity.

The functions of EETs are complex and not yet fully understood. Studies indicate that EETs activate K^+ channels and possess anti-inflammatory effects (Mule et al., 2017; Node et al., 1999). Additionally, EETs may operate through membrane receptor mechanisms, initiated by their binding to plasma membrane EET receptors, which subsequently activate signaling pathways such as the Mitogen-activated protein kinase (MAPK) pathway (Spector and Norris, 2007; Seubert

et al., 2004). Furthermore, EETs have been shown to inhibit pathological endoplasmic reticulum (ER) stress responses and reduce oxidative stress (Batchu et al., 2012). ERK1/2 has been identified as a key downstream molecule responsive to ER stress and plays a role in the cellular defense against such stress (Kurita et al., 2016; Lee and Kim, 2021). In this study, we observed a significant increase in the expression levels of ERK1/2 following TPPU administration, suggesting that the cellular mechanisms of EETs may involve the ERK1/2 pathway, contributing to the anti-seizure effects of TPPU.

5. Conclusion

In this study, we demonstrated that inhibiting sEH with TPPU increased the levels of EETs and other EpFAs, as well as the expression of ERK1/2, in the hippocampus of the LiCl-pilocarpine-induced post-SE rat model. These findings suggest that the cellular mechanism of EETs through the ERK1/2 pathway may be responsible for the anti-seizure effects of TPPU.

Ethical declarations

All procedures were compliant with the requirements from the Animal Ethics Committee of Zhongshan Hospital, Fudan University.

Funding

This work is supported by the project grant from Science and Technology Plan Project of Fujian Province, China (2021GGB033) and Chun-Shen Pyramid Talent Leading Program of Minhang District, Shanghai, China (2023).

CRediT authorship contribution statement

Weifeng Peng: Writing – original draft, Methodology, Investigation, Funding acquisition, Data curation, Conceptualization. **Yijun Shen:** Investigation, Methodology. **Xin Wang:** Supervision. **Zihan Hu:** Investigation, Methodology.

Declaration of Competing Interest

The authors declare that the research was conducted in the absence of any commercial or financial relationships that could be construed as a potential conflict of interest.

Acknowledgements

We extend our heartfelt gratitude to Prof. Bruce D. Hammock at UC Davis for providing TPPU and to Prof. Junyan Liu at Chongqing Medical University for offering technical guidance in measuring EETs.

Author Contributions

WP designed the experiment, completed reanalysis of article data, and wrote the manuscript. ZH and YS performed parts of the animal experiment. XW instructed the study.

Consent to Participate

Not applicable.

Consent for Publication

Not applicable.

Data Availability

The raw data supporting the conclusions of this article will be made available by the authors, without undue reservation.

References

- Ahmedov, M.L., Kemerdere, R., Baran, O., Inal, B.B., Gumus, A., Coskun, C., Yeni, S.N., Eren, B., Uzan, M., Tanriverdi, T., 2017. Tissue expressions of soluble human epoxide hydrolase-2 enzyme in patients with temporal lobe epilepsy. *World Neurosurg.* 106, 46–50. <https://doi.org/10.1016/j.wneu.2017.06.137>.
- Batchu, S.N., Lee, S.B., Samokhvalov, V., Chaudhary, K.R., El-Sikhry, H., Weldon, S.M., Seubert, J.M., 2012. Novel soluble epoxide hydrolase inhibitor protects mitochondrial function following stress. *Can. J. Physiol. Pharm.* 90 (6), 811–823. <https://doi.org/10.1139/y2012-082>.
- Bianco, R.A., Agassandian, K., Cassell, M.D., Spector, A.A., Sigmund, C.D., 2009. Characterization of transgenic mice with neuron-specific expression of soluble epoxide hydrolase. *Brain Res* 1291, 60–72. <https://doi.org/10.1016/j.brainres.2009.07.060>.
- Butler, T., Li, Y., Tsui, W., Friedman, D., Mao, A., Wang, X., Harvey, P., Tanzi, E., Morim, S., Kang, Y., Mosconi, L., Talos, D., Kuzniecky, R., Vallhabjousla, S., Thesen, T., Glodzik, L., Ichise, M., Silbersweig, D., Stern, E., de Leon, M.J., French, J., 2016. Transient and chronic seizure-induced inflammation in human focal epilepsy. *Epilepsia* 57 (9), e191–e194. <https://doi.org/10.1111/epi.13457>.
- Grinan-Ferre, C., Codony, S., Pujol, E., Yang, J., Leiva, R., Escolano, C., Puigoriol-Illamola, D., Companys-Aleman, J., Corpas, R., Sanfeliu, C., Perez, B., Loza, M.L., Brea, J., Morisseau, C., Hammock, B.D., Vazquez, S., Pallas, M., Galdeano, C., 2020. Pharmacological inhibition of soluble epoxide hydrolase as a new therapy for Alzheimer's disease. *Neurotherapeutics*. <https://doi.org/10.1007/s13311-020-00854-1>.
- Hashimoto, K., 2019. Role of soluble epoxide hydrolase in metabolism of PUFAs in psychiatric and neurological disorders. *Front Pharm.* 10, 36. <https://doi.org/10.3389/fphar.2019.00036>.
- Hu, J., Dziumbala, S., Lin, J., Bibli, S.I., Zukunft, S., de Mos, J., Awwad, K., Fromel, T., Jungmann, A., Devraj, K., Cheng, Z., Wang, L., Fauser, S., Eberhart, C.G., Sodhi, A., Hammock, B.D., Liebner, S., Muller, O.J., Glaubit, C., Hammes, H.P., Popp, R., Fleming, I., 2017. Inhibition of soluble epoxide hydrolase prevents diabetic retinopathy. *Nature* 552 (7684), 248–252. <https://doi.org/10.1038/nature25013>.
- Hung, Y.W., Hung, S.W., Wu, Y.C., Wong, L.K., Lai, M.T., Shih, Y.H., Lee, T.S., Lin, Y.Y., 2015. Soluble epoxide hydrolase activity regulates inflammatory responses and seizure generation in two mouse models of temporal lobe epilepsy. *Brain Behav. Immun.* 43, 118–129. <https://doi.org/10.1016/j.bbi.2014.07.016>.
- Illif, J.J., Jia, J., Nelson, J., Goyagi, T., Klaus, J., Alkayed, N.J., 2010. Epoxyeicosanoid signaling in CNS function and disease. *Prostaglandins Other Lipid Mediat* 91 (3–4), 68–84. <https://doi.org/10.1016/j.prostaglandins.2009.06.004>.
- Inceoglu, B., Zolkowska, D., Yoo, H.J., Wagner, K.M., Yang, J., Hackett, E., Hwang, S.H., Lee, K.S., Rogawski, M.A., Morisseau, C., Hammock, B.D., 2013. Epoxy fatty acids and inhibition of the soluble epoxide hydrolase selectively modulate GABA mediated neurotransmission to delay onset of seizures. *PLoS One* 8 (12), e80922. <https://doi.org/10.1371/journal.pone.0080922>.
- Josephson, C.B., Lowerison, M., Vallerand, I., Sajobi, T.T., Patten, S., Jette, N., Wiebe, S., 2017. Association of depression and treated depression with epilepsy and seizure outcomes: a multicohort analysis. *JAMA Neurol.* 74 (5), 533–539. <https://doi.org/10.1001/jamaneurol.2016.5042>.
- Kihara, Y., 2020. Introduction: druggable lipid signaling pathways. *Adv. Exp. Med. Biol.* 1274, 1–4. https://doi.org/10.1007/978-3-030-50621-6_1.
- Kurita, H., Okuda, R., Yokoo, K., Inden, M., Hozumi, I., 2016. Protective roles of SLC30A3 against endoplasmic reticulum stress via ERK1/2 activation. *Biochem Biophys. Res. Commun.* 479 (4), 853–859. <https://doi.org/10.1016/j.bbrc.2016.09.119>.
- Lee, D.S., Kim, J.E., 2021. Regional specific activations of ERK1/2 and CDK5 differently regulate astroglial responses to ER stress in the rat hippocampus following status epilepticus. *Brain Res.* 1753, 147262. <https://doi.org/10.1016/j.brainres.2020.147262>.
- Liu, J.Y., Lin, Y.P., Qiu, H., Morisseau, C., Rose, T.E., Hwang, S.H., Chiamvimonvat, N., Hammock, B.D., 2013. Substituted phenyl groups improve the pharmacokinetic profile and anti-inflammatory effect of urea-based soluble epoxide hydrolase inhibitors in murine models. *Eur. J. Pharm. Sci.* 48 (4–5), 619–627. <https://doi.org/10.1016/j.ejps.2012.12.013>.
- Luo, Y., Wang, L., Peng, A., Liu, J.Y., 2019. Metabolic profiling of human plasma reveals the activation of 5-lipoxygenase in the acute attack of gouty arthritis. *Rheumatol. (Oxf.)* 58 (2), 345–351. <https://doi.org/10.1093/rheumatology/key284>.
- Luo, Y., Wu, M.Y., Deng, B.Q., Huang, J., Hwang, S.H., Li, M.Y., Zhou, C.Y., Zhang, Q.Y., Yu, H.B., Zhao, D.K., Zhang, G., Qin, L., Peng, A., Hammock, B.D., Liu, J.Y., 2019. Inhibition of soluble epoxide hydrolase attenuates a high-fat diet-mediated renal injury by activating PAX2 and AMPK. *Proc. Natl. Acad. Sci. USA* 116 (11), 5154–5159. <https://doi.org/10.1073/pnas.1815746116>.
- Ma, M., Ren, Q., Yang, J., Zhang, K., Xiong, Z., Ishima, T., Pu, Y., Hwang, S.H., Toyoshima, M., Iwayama, Y., Hisano, Y., Yoshikawa, T., Hammock, B.D., Hashimoto, K., 2019. Key role of soluble epoxide hydrolase in the neurodevelopmental disorders of offspring after maternal immune activation. *Proc. Natl. Acad. Sci. USA* 116 (14), 7083–7088. <https://doi.org/10.1073/pnas.1819234116>.
- Morisseau, C., Hammock, B.D., 2005. Epoxide hydrolases: mechanisms, inhibitor designs, and biological roles. *Annu Rev. Pharm. Toxicol.* 45, 311–333. <https://doi.org/10.1146/annurev-pharmtox.45.120403.095920>.
- Morisseau, C., Hammock, B.D., 2013. Impact of soluble epoxide hydrolase and epoxyeicosanoids on human health. *Annu Rev. Pharm. Toxicol.* 53, 37–58. <https://doi.org/10.1146/annurev-pharmtox-011112-140244>.
- Mule, N.K., Orjuela Leon, A.C., Falck, J.R., Arand, M., Marowsky, A., 2017. 11,12-Epoxyeicosatrienoic acid (11,12 EET) reduces excitability and excitatory transmission in the hippocampus. *Neuropharmacology* 123, 310–321. <https://doi.org/10.1016/j.neuropharm.2017.05.013>.
- Node, K., Huo, Y., Ruan, X., Yang, B., Spiecker, M., Ley, K., Zeldin, D.C., Liao, J.K., 1999. Anti-inflammatory properties of cytochrome P450 epoxygenase-derived eicosanoids. *Science* 285 (5431), 1276–1279. <https://doi.org/10.1126/science.285.5431.1276>.
- Paudel, Y.N., Shaikh, M.F., Shah, S., Kumari, Y., Othman, I., 2018. Role of inflammation in epilepsy and neurobehavioral comorbidities: Implication for therapy. *Eur. J. Pharm.* 837, 145–155. <https://doi.org/10.1016/j.ejphar.2018.08.020>.
- Peng, W.F., Ding, J., Li, X., Fan, F., Zhang, Q.Q., Wang, X., 2016. N-methyl-D-aspartate receptor NR2B subunit involved in depression-like behaviours in lithium chloride-pilocarpine chronic rat epilepsy model. *Epilepsy Res* 119, 77–85. <https://doi.org/10.1016/j.eplepsyres.2015.09.013>.
- Racine, R.J., 1972. Modification of seizure activity by electrical stimulation. II. Motor seizure. *Electro Clin. Neurophysiol.* 32 (3), 281–294. [https://doi.org/10.1016/0013-4694\(72\)90177-0](https://doi.org/10.1016/0013-4694(72)90177-0).
- Ren, Q., Ma, M., Ishima, T., Morisseau, C., Yang, J., Wagner, K.M., Zhang, J.C., Yang, C., Yao, W., Dong, C., Han, M., Hammock, B.D., Hashimoto, K., 2016. Gene deficiency and pharmacological inhibition of soluble epoxide hydrolase confers resilience to repeated social defeat stress. *Proc. Natl. Acad. Sci. USA* 113 (13), E1944–E1952. <https://doi.org/10.1073/pnas.1601532113>.
- Seubert, J., Yang, B., Bradbury, J.A., Graves, J., Degraff, L.M., Gabel, S., Gooch, R., Foley, J., Newman, J., Mao, L., Rockman, H.A., Hammock, B.D., Murphy, E., Zeldin, D.C., 2004. Enhanced postsynaptic functional recovery in CYP2J2 transgenic hearts involves mitochondrial ATP-sensitive K⁺ channels and p42/p44 MAPK pathway. *Circ. Res* 95 (5), 506–514. <https://doi.org/10.1161/01.RES.0000139436.89654.c8>.
- Shen, Y., Peng, W., Chen, Q., Hammock, B.D., Liu, J., Li, D., Yang, J., Ding, J., Wang, X., 2019. Anti-inflammatory treatment with a soluble epoxide hydrolase inhibitor attenuates seizures and epilepsy-associated depression in the LiCl-pilocarpine post-status epilepticus rat model. *Brain Behav. Immun.* 81, 535–544. <https://doi.org/10.1016/j.bbi.2019.07.014>.
- Spector, A.A., Norris, A.W., 2007. Action of epoxyeicosatrienoic acids on cellular function. *Am. J. Physiol. Cell Physiol.* 292 (3), C996–C1012. <https://doi.org/10.1152/ajpcell.00402.2006>.
- Sura, P., Sura, R., Enayetallah, A.E., Grant, D.F., 2008. Distribution and expression of soluble epoxide hydrolase in human brain. *J. Histochem Cytochem* 56 (6), 551–559. <https://doi.org/10.1369/jhc.2008.950659>.
- Swardfager, W., Hennebelle, M., Yu, D., Hammock, B.D., Levitt, A.J., Hashimoto, K., Taha, A.Y., 2018. Metabolic/inflammatory/vascular comorbidity in psychiatric disorders; soluble epoxide hydrolase (sEH) as a possible new target. *Neurosci. Biobehav. Rev.* 87, 56–66. <https://doi.org/10.1016/j.neubiorev.2018.01.010>.
- Ulu, A., Inceoglu, B., Yang, J., Singh, V., Vito, S., Wulff, H., Hammock, B.D., 2016. Inhibition of soluble epoxide hydrolase as a novel approach to high dose diazepam induced hypotension. *J. Clin. Toxicol.* 6 (3). <https://doi.org/10.4172/2161-0495.1000300>.
- Vezzani, A., Balosso, S., Ravizza, T., 2008. The role of cytokines in the pathophysiology of epilepsy. *Brain Behav. Immun.* 22 (6), 797–803. <https://doi.org/10.1016/j.bbi.2008.03.009>.
- Vezzani, A., Friedman, A., Dingledine, R.J., 2013. The role of inflammation in epileptogenesis. *Neuropharmacology* 69, 16–24. <https://doi.org/10.1016/j.neuropharm.2012.04.004>.
- Vito, S.T., Austin, A.T., Banks, C.N., Inceoglu, B., Bruun, D.A., Zolkowska, D., Tancredi, D.J., Rogawski, M.A., Hammock, B.D., Lein, P.J., 2014. Post-exposure

- administration of diazepam combined with soluble epoxide hydrolase inhibition stops seizures and modulates neuroinflammation in a murine model of acute TETS intoxication. *Toxicol. Appl. Pharm.* 281 (2), 185–194. <https://doi.org/10.1016/j.taap.2014.10.001>.
- Wang, Z.H., Mong, M.C., Yang, Y.C., Yin, M.C., 2018. Asiatic acid and maslinic acid attenuated kainic acid-induced seizure through decreasing hippocampal inflammatory and oxidative stress. *Epilepsy Res* 139, 28–34. <https://doi.org/10.1016/j.eplepsyres.2017.11.003>.
- Zarriello, S., Tuazon, J.P., Corey, S., Schimmel, S., Rajani, M., Gorsky, A., Incontri, D., Hammock, B.D., Borlongan, C.V., 2019. Humble beginnings with big goals: Small molecule soluble epoxide hydrolase inhibitors for treating CNS disorders. *Prog. Neurobiol.* 172, 23–39. <https://doi.org/10.1016/j.pneurobio.2018.11.001>.